

Supplemental Information

Impaired Lysosomal Function Entails Monoclonal Light Chain Renal Fanconi Syndrome

Alessandro Luciani, Christophe Sirac, Sara Terryn, Vincent Javaugue, Jenny Ann Prangue, Sébastien Bender, Amélie Bonaud, Michel Cogné, Pierre Aucouturier, Pierre Ronco, Frank Bridoux and Olivier Devuyst

Detailed Material and Methods

References

Supplementary Figure Legends

Supplementary Table 1

Supplementary Figures S1-S6

Detailed Materials and Methods

Mouse models. Experiments were conducted on age (16-20 weeks) and gender-matched wild-type (WT), κ DE and κ CH transgenic mice generated as previously described (1). The κ DE mice were obtained using the same strategy than κ CH mice, with targeted insertion in the κ locus leading to the production of a hybrid LC formed of a human V domain associated with the murine constant κ region. The V domain is derived from the V κ 1-33 germline gene (2), and was extracted as previously described (3) from a patient diagnosed with AL amyloidosis. All experiments were conducted in mice homozygous for the targeted insertion which does not enable the production of endogenous κ LCs. The LC production in urine was measured by ELISA as previously described (1). Mice were maintained under temperature- and humidity-controlled conditions with 12-h light/12-h dark cycles with free access to appropriate standard diet (Carfil Quality, Oud-Turnhout, Belgium). The experiments were conducted in accordance with the National Institutes of Health Guide for the Care and Use of Laboratory Animals and were approved by the Ethics Committees of the Université catholique de Louvain, the Université de Limoges and the University of Zurich.

Renal function parameters. After appropriate training, mice were placed overnight in metabolic cages with ad libitum access to food and drinking water; urine was collected over ice and diuresis was measured. Blood was obtained by puncture of the vena cava at the time of euthanasia with ketamine/xylazine or isoflurane (4). The urine and blood parameters were measured using a SynchronCX5 analyzer (Beckman Coulter, Fullerton, CA, USA), whereas Clara cell protein (CC16) concentration was measured in duplicate by latex immunoassay (courtesy of X. Dumont, UCL Medical School, Brussels, Belgium). Urinary LMW proteins, including vitamin D-binding protein and transferrin were measured by western blotting as described previously (4,5). The kidneys were carefully dissected and harvested. One kidney was split transversally and one half was fixed for histology or immunostaining while the other half was flash-frozen and stored at -80°C. The contralateral kidney was taken for primary cultures of proximal tubule cells or for whole kidney RNA extraction.

Histological analysis. Light microscopic examination was performed on kidney samples stained with either hematoxylin/eosin (HES), Periodic Acid Schiff, light green trichrome, silver methenamine, or toluidine blue as previously described (1,4,6). Regular procedures were performed on paraffin-embedded, 6 μ m-thick sections. For semi-thin sections, tissue was

post-fixed for 1 h in 1% osmium tetroxide in PBS (Life Technologies, Zug, Switzerland), dehydrated in serial ethanol solutions and embedded in an araldite-epon mixture. Embedded tissues were then placed at 60°C for 2 days to polymerize. Semithin, 1 µm-thick sections were prepared with an ultramicrotome and stained with toluidine blue and examined under light microscope.

Electron microscopy and immunogold analysis. For ultrastructural examination, kidney tissue and proximal tubule cell monolayers were fixed 2.5% glutaraldehyde in 125 mM cacodylate buffer and stained with uranyl acetate and lead citrate and examined with a JEOL 1010 transmission electron microscope (Tokyo, Japan). For immuno-electron microscopy, kidney samples were fixed with a mixture of 4% (w/v) PFA and 0.05% (v/v) glutaraldehyde in 0.2 M HEPES (pH 7.4) for 15 min at room temperature and then placed in 4% (w/v) PFA in the same buffer for 30 min at room temperature. After washing, samples were incubated with blocking buffer for 30 min at room temperature and then with the primary antibody (diluted in blocking buffer) overnight at 4°C. Next, samples were washed in PBS and incubated with a secondary antibody coupled to 1.4-nm gold particles. After extensive washing with PBS, samples were post-fixed in 1% glutaraldehyde in 0.2 M HEPES (pH=7.4) for 5 min. The gold particles were enhanced by Goldenhance-EM (NanoProbes, Yaphank, NY, USA) following the manufacturer's instructions. After washing, the samples were treated with 1% osmium tetroxide plus 1.5% potassium ferrocyanide in 0.1 M cacodylate buffer (pH 7.3) for 2 h on ice in the dark; they were then dehydrated, embedded in Epoxy resin (Sigma-Aldrich, Buchs, Switzerland) and polymerized for at least 24 h at 62°C. Sections were analyzed at 120 kV using a Tecnai 12 electron microscope (Hillsboro, OR, USA).

Antibodies and reagents. The following antibodies were used in this study: Rat anti-κLC (Beckman Coulter, Villepinte, France); mouse anti-PCNA (Dako, Glostrup, Denmark); rabbit anti-DBP (Dako); rabbit anti-LMW proteins (Dako); rabbit anti-CC16 (BioVendor, Heidelberg, Germany); rabbit anti-transferrin (Dako); mouse anti-β-actin (Sigma, St. Louis, USA); rabbit anti-ZONAB (Invitrogen; Bethyl, Montgomery, TX, USA); rabbit anti-AQP1 (Millipore, Billerica, MA, USA); rabbit anti-CD13 (Abcam, Cambridge, UK); mouse anti-p84 (Abcam); rabbit anti-LAMP1 (Abcam); rabbit anti-LAMP2 (Abcam); goat anti-cathepsin-D (Santa Cruz Biotechnology); rabbit anti-Rab5 (Cell Signaling Technology, Leiden, The Netherlands); rabbit anti-Rab7 (Santa Cruz Biotechnology); mouse anti-GM130 (Abcam);

and rabbit anti-EEA-1 (Cell Signaling). Sheep anti-megalin and rabbit anti-cubilin antibodies were kindly provided by Dr. P. Verroust and Dr. R. Kozyraki (INSERM, Paris, France). Compounds included bafilomycin-A1 (Enzo Life Sciences, Lausen, Switzerland); ammonium chloride (NH₄Cl, Sigma); valinomycin (Life Technologies); methyl- β -cyclo-dextrin (Sigma); filipin (Sigma); and nocodazole (Enzo Life Sciences).

Characteristics, production, purification and digestion of human κ LCs. Human LC genes were isolated and transfected in the hybridoma cell line SP2/0 as previously described (6). The human κ LCs were produced by the SP2/0 cell line, a B cell hybridoma lacking endogenous Ig and constitutively overexpressing human LCs from patients with biopsy-proven renal Fanconi syndrome (κ CH and κ DU), renal AL amyloidosis (κ DE) or cast nephropathy (κ RO). The characteristics of the human LCs used in this study are depicted in Table 2. Theoretical isoelectric point (*pI*) was estimated using the Protein calculator v3.4 software (<http://protcalc.sourceforge.net/>). Prediction of aggregating regions in V domain was calculated using the TANGO algorithm (<http://tango.crg.es/protected/academic/calculation.jsp>) (7). Molecular modelling of the κ LCs was performed using VMD software (<http://www.ks.uiuc.edu/Research/vmd/>) (8) with the pdb files obtained from the Swiss-Model server (<http://swissmodel.expasy.org/>) (9) using the 2bx5l crystal structure as template. The κ LCs were highly enriched using a Celine disposable bioreactor system (Integra Biosciences AG, Zizers, Switzerland), all with the same conditions precluding phenotypical differences due to residual FBS or other associated proteins. For κ LCs uptake experiments, cell supernatants containing human κ LCs were directly diluted in serum free, culture medium to the final concentration of 25 μ g/mL before being exposed to mPTCs. For cathepsin-B digestion experiments, κ LCs were purified on HiTrap Protein L columns (GE healthcare, Glattbrugg, Switzerland), concentrated at 1mg/mL by Amicon® Ultra Centrifugal Filters (Millipore, Molsheim, France) and were digested by cathepsin-B at 37°C as previously described (10). Samples were analyzed by western blot using a mouse anti-human V κ 1 antibody (kindly provided by Alan Solomon).

Isolation and primary cultures of proximal tubule cells. Primary cultures of mouse PT cells (mPTCs) were prepared from male C57/BL6 mice as described previously (4, 11). Freshly micro-dissected PT segments were seeded onto collagen-coated chamber slides (Nunc, Rochester, NY, USA) or collagen coated 24-well plates (Corning, Tewksbury, MA, USA) and

cultured at 37°C and 5% CO₂ in DMEM/F12 with 0.5% dialyzed FBS, 15nM HEPES, 0.55 mM sodium pyruvate, 0.1ml/L non-essential amino acids, hydrocortisone, hEGF, epinephrine, insulin, triiodothyronine, TF, and gentamicin/amphotericin. The medium was replaced every 48 h. Confluent monolayers of mPTCs expanded from the tubular fragments after 6–7 days, characterized by a high endocytic uptake capacity. All experiments were performed on non-passaged, confluent monolayers grown on chamber slides or plates.

Human κLCs uptake. For the uptake of all human κLCs, primary mPTCs were plated in culture medium, briefly rinsed, and then cultured for 4h in serum-free, HEPES-buffered DMEM/F12. The cells were then incubated with 25µg/mL of human κLCs in serum-free, HEPES-buffered DMEM/F12 for 60 min at 4°C and chased in κLCs-free, complete medium for the indicated times at 37°C, before being processed for western blotting or immunofluorescence analyses. Each incubation could be done using a different, non-pooled monoclonal κLC.

Endocytosis assays. For endocytic uptake assays, mPTCs cells were incubated for 60 min at 4°C with 100 µg/mL Bovine Serum Albumin (BSA)-Alexa-Fluor-488 or with 50 µg/mL Transferrin (Tf)-Alexa-Fluor-546 (both from Life Technologies). The cells were given an acid wash and warmed to 37°C in growth cell medium for 15 min before being fixed and processed for immunofluorescence analyses (4).

Quantitative real-time PCR. Total RNA was extracted from kidneys using Aurum™ Total RNA Fatty and Fibrous Tissue Kit (Bio-Rad, Hercules, CA), following the manufacturers protocol. DNase I treatment was performed to eliminate genomic DNA contamination. Total RNA was extracted from primary cell cultures with RNAqueousR kit (Applied Biosystems, Life Technologies), following the manufacturers protocol. One microgram of RNA was used to perform the reverse transcriptase reaction with iScript™ cDNA Synthesis Kit (Bio-Rad). The primers were designed using Beacon Designer 2.0 (Premier Biosoft International, Palo Alto, USA) ([Suppl. Table 1](#)). Changes in target genes mRNA levels were determined by quantitative reverse transcriptase polymerase chain reaction (RT-PCR) with an iCycler IQ System (Bio-Rad) using SYBR Green I detection of single PCR product accumulation. The qRT-PCR analyses were performed in duplicate with 100nM of both sense and anti-sense primers in a final volume of 20 µl using iQ™ SYBR Green Supermix (Bio-Rad). PCR conditions were 94°C for 3 min followed by 40 cycles of 30 s at 95°C, 30 s at 61°C and 1 min

at 72°C. The relative changes in target gene/GAPDH mRNA ratio were determined by the relation $2^{-\Delta\Delta Ct}$ (4).

Subcellular fractionation. For subcellular fractionation, kidney cortex samples were dissected in ice-cold dissection solution (HBSS with in mmol/l: 10 glucose, 5 glycine, 1 alanine, 15 HEPES, pH 7.4 and osmolality 325 mosmol/kgH₂O), and homogenized by Dounce homogenizer in five volumes of TBS with 10% sucrose, protease inhibitor and phosphatase inhibitors (Complete Mini^R, Roche Diagnostics, Rotkreuz, Switzerland). The mixture was centrifuged at 800×g for 5 min. The supernatant represented total fraction while pellet (nuclear fraction) was washed twice and lysed in 0.5 Triton X-100 buffer 0.5% SDS and sonicated. All the above procedures prior to boiling in SDS-sample loading buffer were carried out either on ice or at 4°C. The total and nuclear fractions were analyzed by SDS-PAGE and immunoblotting.

Western blotting. Immunoblotting was performed as described previously (4). Proteins were extracted from isolated kidneys or primary cultured cells, lysed in lysis buffer containing protease inhibitors, followed by sonication and centrifugation at 16,000 g for 1 min at 4°C. The samples were thawed on ice, normalized for protein (20µg/lane) or urinary creatinine levels, diluted in Laemmli buffer and separated by SDS-PAGE in reducing conditions. After blotting onto nitrocellulose and blocking, membranes were incubated overnight at 4°C with primary antibody, washed, incubated with peroxidase-labeled secondary antibody, and visualized with enhanced chemiluminescence (ECL Pierce, Life Technologies). For re-probing, the membranes were rinsed, incubated for 30 min at 55°C in a stripping buffer (62.5 mmol/l Tris-HCl, 2% SDS, 100 mM - mercaptoethanol, pH 7.4), before incubation with primary antibodies. Quantitative analysis was performed by scanning the blots and measuring the relative density of each band normalized to β-actin using NIH-Image V1-57 software.

Immunofluorescence and confocal microscopy. Mouse kidneys were snap-frozen in cryogenic Tissue-Tek OCT compound (Electron Microscopy Sciences, Hatfield, USA). The embedded tissue was sectioned at 6 µm with a Leica cryostat (Leica, Heerbrugg, Switzerland). The sections were fixed with 4% paraformaldehyde, blocked with PBS containing 5% BSA, and incubated for 1 h with primary antibodies. After three PBS rinses, fluorophore-conjugated Alexa secondary antibodies (Invitrogen) were applied for 30 min. Sections were subsequently mounted in Prolong Gold Anti-fade reagent (Invitrogen) and then

analyzed under a Leica SP5 confocal laser scanning microscope (Center for Microscopy and Image Analysis, University of Zurich).

The cells on chamber slides were fixed for 10 min with 4% paraformaldehyde (Sigma) in PBS, quenched with 50 mM NH₄Cl and permeabilized for 30 min in blocking buffer (0.1% (w/v) Triton X-100, 0.5% (w/v) BSA in PBS/Ca/Mg). The cells were incubated for 2 h with the primary antibody, washed three times in PBS, incubated for 1 h with the secondary (Alexa labelled) antibody, washed three times in PBS and were finally mounted on Vectashield covered coverslips (Vector Laboratories, Burlingame, CA, USA). The samples were examined under Leica SP5 confocal laser scanning microscope equipped with ×63 oil-immersion objective. Image processing was done with Adobe Photoshop C2 (Adobe System Inc, San Jose, USA). To perform quantitative image analysis, 10–15 randomly chosen fields that included 8–10 cells each were scanned, using the same setting parameters (i.e. pinhole, laser power, and offset gain and detector amplification) below pixel saturation. The correlation coefficient analysis was used as value of co-localization as previously described (14). Quantification of the number and size of LAMP1-positive vesicles was performed using the AnalySIS software (Soft Imaging Systems GmbH, Muenster, Germany). Quantification was carried out on at least 200 cells per condition, obtained from 2 to 4 independent experiments.

Quantification of lysosome distribution. To score lysosome distribution, mPTCs were categorized into perinuclear-dominant lysosomal pattern (more than 50% of LAMP1-positive vesicles localized in the perinuclear region) and peripheral-dominant pattern (more than 50% of the vesicles localized in the peripheral region), on the basis of the number of lysosomes in each region (12). The data are expressed as a proportion of cells with predominantly (50%) perinuclear lysosomes. Quantification was carried out on at least 200 cells per condition from 2 to 4 independent experiments.

Lysosomal pH measurement. LysoSensor Blue DND-167 is commonly used to measure the pH of acidic organelles including lysosomes (13). Briefly, cells were loaded with 1 μM LysoSensor Green DND-167 (Life Technologies) in pre-warmed regular medium for 20 min at 37°C. Then the cells were washed twice with PBS, fixed and stained with LAMP1 antibody and analyzed by confocal microscope. The correlation coefficient analysis was used as value of co-localization between LysoSensor and LAMP1 as previously described (14)

Quantification of lysosomal pH was performed using a ratiometric lysosomal pH dye, LysoSensor Yellow/Blue DND-160 (Life Technologies), as described previously (13). Briefly, cells were trypsinized and labeled with 2mM LysoSensor Yellow/Blue DND-160 for 30 min at 37°C in regular medium, and excessive dye was washed out using PBS. The labeled cells were treated for 10 min with 10mM monensin (Sigma) and 10 M nigericin (Sigma) in 25 mM 2-(N-morpholino) ethanesulfonic acid (MES) calibration buffer, pH 3.5–6.0, containing 5 mM NaCl, 115 mM KCl and 1.2 mM MgSO₄. Quantitative comparisons were performed in a 96-well plate, and the fluorescence was measured with a micro-plate reader at 37°C. Light emitted at 440 and 535 nm in response to excitation at 340 and 380 nm were measured, respectively. The ratio of light emitted with 340 and 380 nm excitation was plotted against the pH values in MES buffer, and the pH calibration curve for the fluorescence probe was generated from the plot using Microsoft Excel.

TUNEL assay. Apoptotic cell death was measured by using Click-iT TUNEL Alexa Fluor 488 imaging assay kit according to the manufacturer's instructions (Molecular Probes, Life Technologies).

Statistical analysis. Data were statically analyzed using Prism5 (GraphPad Software, La Jolla, CA, USA). Two-tailed Student's *t* test or one-way ANOVA followed by post-hoc tests were used to assess the statistical value of differences between groups. Results are presented as mean ± SEM. A *P* value < 0.05 was considered significant.

References

1. Sirac C, Bridoux F, Carrion C, Devuyst O, Fernandez B, Goujon J-M, El Hamel C, Aldigier J-C, Touchard G, Cogné M: Role of the monoclonal kappa chain V domain and reversibility of renal damage in a transgenic model of acquired Fanconi's syndrome. *Blood* 108: 536-544, 2006
2. Messiaen T, Deret S, Mougnot B, Bridoux F, Dequiedt P, Dion JJ, Makdassi R, Meeus F, Pourrat J, Touchard G, Vanhille P, Zaoui P, Aucouturier P, Ronco PM: Adult Fanconi syndrome secondary to light chain gammopathy. Clinicopathologic heterogeneity and unusual features in 11 patients. *Medicine (Baltimore)* 79: 135-154, 2000
3. Bridoux F, Sirac C, Hugue V, Decourt C, Thierry A, Quellard N, Abou-Ayache R, Goujon JM, Cogné M, Touchard G: Fanconi's syndrome induced by a monoclonal κ 3 light chain in Waldenstrom's macroglobulinemia. *Am J Kidney Dis* 45:749-757, 2005
4. Raggi C, Luciani A, Nevo N, Antignac C, Terryn S, Devuyst O: Dedifferentiation and aberrations of the endolysosomal compartment characterize the early stage of nephropathic cystinosis. *Hum Mol Genet* 23: 2266-2278, 2014
5. Christensen EI, Devuyst O, Dom G, Nielsen R, Van der Smissen P, Verroust P, Leruth M, Guggino WB, Courtoy PJ: Loss of chloride channel CLC-5 impairs endocytosis by defective trafficking of megalin and cubilin in kidney proximal tubules. *Proc Natl Acad Sci USA* 100: 8472-8477, 2003
6. Decourt C, Rocca A, Bridoux F, Vrtovsnik F, Preud'homme JL, Cogné M, Touchard G: Mutational analysis in murine models for myeloma-associated Fanconi's syndrome or cast myeloma nephropathy. *Blood* 94: 3559-3566, 1999
7. Linding R, Schymkowitz J, Rousseau F, Diella F, Serrano L. A comparative study of the relationship between protein structure and beta-aggregation in globular and intrinsically disordered proteins. *J Mol Biol* 342: 345-353, 2004
8. Humphrey W, Dalke A, Schulten K: VMD: visual molecular dynamics. *J Mol Graph* 14: 33-38, 1996
9. Arnold K, Bordoli L, Kopp J, Schwede T: The SWISS-MODEL workspace: a web-based environment for protein structure homology modelling. *Bioinformatics* 22: 195-201, 2006

10. Leboulleux M, Lelongt B, Mougenot B, Touchard G, Makdassi R, Rocca A, Noel LH, Ronco PM, Aucouturier P: Protease resistance and binding of Ig light chains in myeloma-associated tubulopathies. *Kidney Int* 48: 72-79, 1995
11. Terryn S, Jouret F, Vandenabeele F, Smolders I, Moreels M, Devuyst O, Steels P, Van Kerkhove E: A primary culture of mouse proximal tubular cells, established on collagen-coated membranes. *Am J Physiol Renal Physiol* 293: F476-F485, 2007
12. Korolchuk VI, Saiki S, Lichtenberg M, Siddiqi FH, Roberts EA, Imarisio S, Jahreiss L, Sarkar S, Futter M, Menzies FM, O'Kane CJ, Deretic V, Rubinsztein DC: Lysosomal positioning coordinates cellular nutrient responses. *Nat Cell Biol* 13: 453-460, 2011
13. Lee J-H, Yu WH, Kumar A, Lee S, Mohan PS, Peterhoff CM, Wolfe DM, Martinez-Vicente M, Massey AC, Sovak G, Uchiyama Y, Westaway D, Cuervo AM, Nixon RA: Lysosomal proteolysis and autophagy require presenilin 1 and are disrupted by Alzheimer-related PS1 mutations. *Cell* 141: 1146-1158, 2010
14. Luciani A, Vilella VR, Esposito S, Brunetti-Pierri N, Medina D, Settembre C, Gavina M, Pulze L, Giardino I, Pettoello-Mantovani M, D'Apolito M, Guido S, Masliah E, Spencer B, Quarantino S, Raia V, Ballabio A, Maiuri L: Defective CFTR induces aggresome formation and lung inflammation in cystic fibrosis through ROS-mediated autophagy inhibition. *Nat Cell Biol* 12: 863-875, 2010

Supplementary Figure Legends

Fig. S1. Quantification of urine free κ LCs, dedifferentiation and proliferation in wild-type and κ DE mice.

(A) ELISAs for the detection of κ LCs in urine samples of wild-type (WT) and transgenic κ CH and κ DE mice. The levels of free LCs were similar in κ CH and κ DE mice ($n = 6$). ** $P < 0.01$; *** $P < 0.0001$; ns, not significant. (B) Immunofluorescence staining for megalin, cubilin and NaPi-IIa (DAPI nuclear counterstain) in WT and κ DE kidneys. Scale bar: 50 μ m. (C) Double immunofluorescence staining for Lotus Tetragonolobus Lectin (LTL, green) and PCNA (red) in WT and κ DE kidneys. Nuclei counterstained with DAPI. Scale bar, 25 μ m. Quantification of LTL-positive cells with nuclear PCNA immunoreactivity showed no significant difference ($n=100$ LTL-positive cells). (D) Double immunofluorescence staining for ZONAB (red) and LTL (green) in WT and κ CH kidneys. Nuclei counterstained with DAPI (blue). Scale bar, 25 μ m. Quantification of LTL-positive cells presenting nuclear ZONAB immunoreactivity showed no significant difference ($n=100$ LTL-positive cells).

Fig. S2. Molecular characteristics and protease resistance of human κ LCs.

(A) 3D structures of wild-type κ CH (red) and mutant κ CHm (blue) were superimposed to show modifications induced by the Ala to Ser mutation at position 30. Total V κ domains representation (left) shows a complete homology between the two LCs even in the CDR1 loop (inset) where the mutation at position 30 is present (ball-and-stick representation). (B) Predicted aggregating regions in the V domains of κ CH and κ CHm as calculated by TANGO algorithm. Arrows indicate the position of the residue 30 mutated in κ CHm. (C) Western blotting analysis of purified κ CH, κ CHm, κ DE and κ DU LCs after digestion by cathepsin-B during the indicated times (10 μ g per lane). The 12 kDa resistant fragments are revealed by an anti-human V κ 1 antibody.

Fig. S3. Inhibition of endocytosis by methyl- β -cyclo-dextrin or filipin prevents the internalization of κ LCs in proximal tubule cells.

(A-G) Primary mPTCs were pretreated with cholesterol binding agent methyl- β -cyclo-dextrin (M- β -CD, 10mM for 1h) or filipin (5 μ g/mL for 1h) and then challenged with 25 μ g/mL of κ RO or κ CH for the indicated times. The cells were fixed, stained with an anti- κ LC antibody and subjected to confocal microscopy analysis. Nuclei counterstained with DAPI (blue). Scale

bar, 10 μ m. Right panel: Quantification of cells containing κ LCs. * P <0.005 vs. untreated, # P <0.003 vs. untreated, n = 200 cells per group.

Fig. S4. Exposure to κ LCs does not impact LAMP1 dynamics at the Golgi or endocytic compartments.

(A-B) Primary mPTCs were initially kept for 4h in serum-free culture medium, then incubated with control medium or 25 μ g/mL of κ LCs for 1h and chased in κ LCs-free culture medium for the indicated times at 37°C. (A) The cells were fixed, co-stained with anti-LAMP1 and anti-Rab5 or anti-Rab7 antibodies and subjected to confocal microscopy. Nuclei counterstained with DAPI (blue). Scale bar, 10 μ m. The cells from (A) were assessed for Rab5/LAMP1 or Rab7/LAMP1 co-localizations (correlation coefficient). n = 100 cells per condition. (B) Effect of pre-incubation with nocodazole (30 μ M, 2h) on immunostaining for LAMP1 (red) and the Golgi marker GM130 (green) in cells exposed to control medium or κ LCs and then chased for 24h. There is no co-localization of LAMP1 clusters with GM130. Nuclei counterstained with DAPI (blue). Scale bar, 10 μ m. The cells from (B) were assessed for LAMP1/GMA130 co-localization (correlation coefficient). n = 100 cells per condition.

Fig. S5. Impaired cathepsin-D activity in proximal tubule cells exposed to specific κ LCs.

Primary mPTCs were initially kept for 4h in serum-free culture medium, then incubated with 25 μ g/mL of κ LCs for 1h and chased in κ LCs-free culture medium for the indicated times at 37°C. After exposure to κ LCs, the cells were loaded with membrane permeable-substrate Bodipy-FL-PepstatinA (PepA, 100nM for 30 min), fixed and subjected to confocal microscopy analysis. Left panel: Bodipy-FL fluorescence staining; right panel: quantification of the number of PepA-positive dots in mPTCs exposed to κ LCs. Scale bar, 10 μ m. * P <0.01 κ CH vs. κ RO, # P <0.005 κ CHm vs. κ CH, ** P <0.003 κ DU vs. κ RO, n = 200 cells per condition.

Fig. S6. Endocytic receptors, transporters and apoptosis in mPTCs exposed to κ LCs.

(A-B) Primary mPTCs were initially kept for 4h in serum-free culture medium, then incubated with 25 μ g/mL of κ LCs for 1h and chased in κ LCs-free culture medium for the indicated times at 37°C. (A) Immunofluorescence staining for megalin (green), cubilin (red) and NaPi-IIa (magenta), showing a decreased expression of the apical receptors and

transporter in cells exposed to κ CH. Nuclei counterstained with DAPI (blue). Scale bar, 10 μ m. **(B)** RFS- κ LCs do not promote apoptosis. Quantification of the percentage of TUNEL-positive cells in comparison with Valinomycin treatment (10nM for 6h): * P <0.01 vs. unexposed cells or cells exposed to κ LCs, n = 200 cells per group.

(C-D) Lack of reversibility of the changes in receptors and endocytosis. Primary mPTCs incubated for 1h at 4°C with 25 μ g/ml of κ CH or κ CHm were chased in κ LCs free, growth cell medium for the indicated times. Confocal microscopy and X-Z side-view of Z-stack **(C)** show a sustained decrease (from 24h to 72h) in expression of megalin at the apical plasma membrane, reflected by a major decrease in Alexa-488-albumin uptake **(D)** in cells exposed to κ CH compared to κ CHm.

Supplementary Table 1. Primers used for quantitative RT-PCR analyses.

Gene products	Forward primers (5'-3')	Reverse primers (5'-3')	PCR products (bps)	Efficiency
<i>Gapdh</i>	TGCACCACCAACTGCTTAGC	GGATGCAGGGATGATGTTCT	176	1.04 ± 0.03
<i>Actb</i>	TGCCCATCTATGAGGGCTAC	CCCGTTCAGTCAGGATCTTC	102	1.03 ± 0.04
<i>Hprt 1</i>	ACATTGTGGCCCTCTGTGTG	TTATGTCCCCCGTTGACTGA	162	0.99 ± 0.01
<i>Ppiase</i>	CGTCTCCTTCGAGCTGTTTG	CCACCCTGGCACATGAATC	139	1.02 ± 0.02
<i>18S</i>	GTAACCCGTTGAACCCATT	CCATCCAATCGGTAGTAGCG	151	0.98 ± 0.02
<i>36B4</i>	CTTCATTGTGGGAGCAGACA	TTCTCCAGAGCTGGGTTGTT	150	1.02 ± 0.02
<i>Cubn</i>	TCATTGGCCTCAGACATTCC	CCCAGACCTTCACAAAGCTG	149	1.04 ± 0.05
<i>Lrp2</i>	CAGTGGATTGGGTAGCAGGA	GCTTGGGGTCAACAACGATA	150	0.99 ± 0.04
<i>Pcna</i>	TTGGAATCCCAGAACAGGAG	ATTGCCAAGCTCTCCACTTG	155	0.97 ± 0.04
<i>Ccnd1</i>	AGCAGAAGTGCGAAGAGGAG	CAAGGGAATGGTCTCCTTCA	149	1.03 ± 0.05
<i>Ybx3</i>	AGGACGCGGAGAAGAAAGTT	ACTTGCGTGGGTTGTTTTTC	153	0.98 ± 0.04
<i>Clen5</i>	TGGAGGAGCCAATCCCTGGTGT	AGAAAGCATCGCTCACACTG	156	0.99 ± 0.02
<i>Atp6v1e1</i>	GGCGCTCAGCGATGCAGATGT	CAAGGCGACCTTTCTCAATG	134	1.05 ± 0.01
<i>Car2</i>	CTTGAAGCACTGCATTCCAT	CACGATCCAGGTCACACATT	154	1.02 ± 0.03

Figure S1

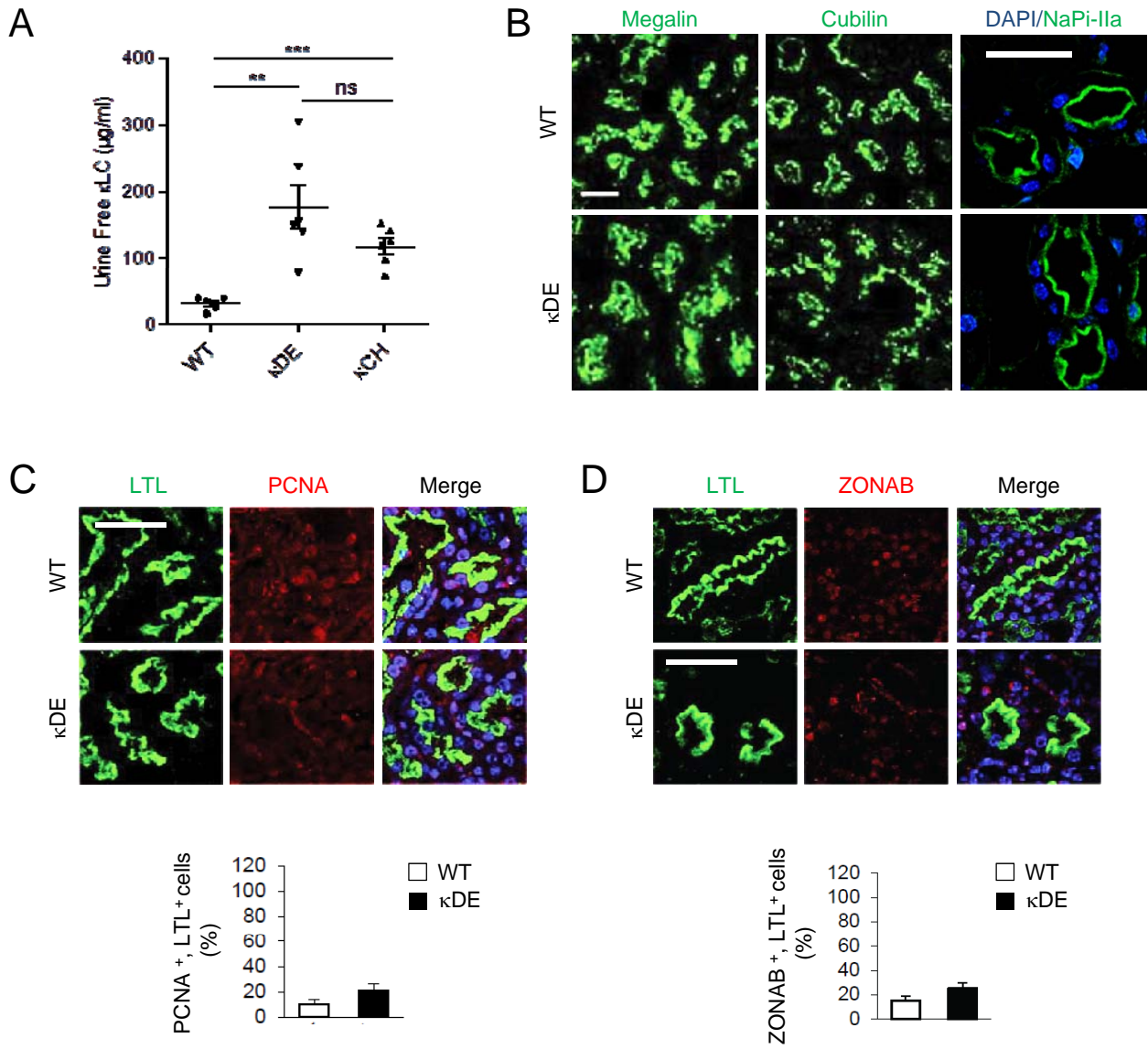
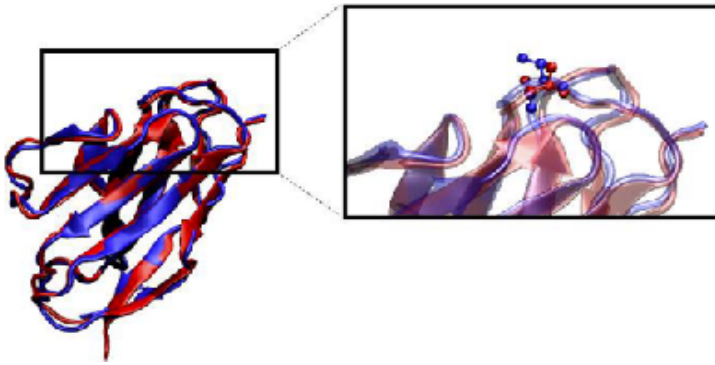
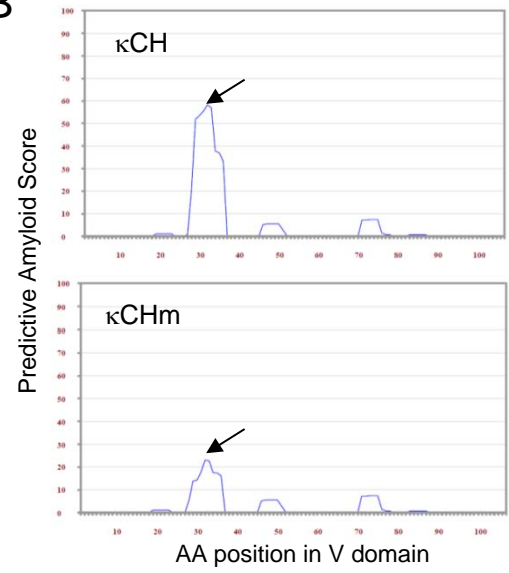


Figure S2

A



B



C

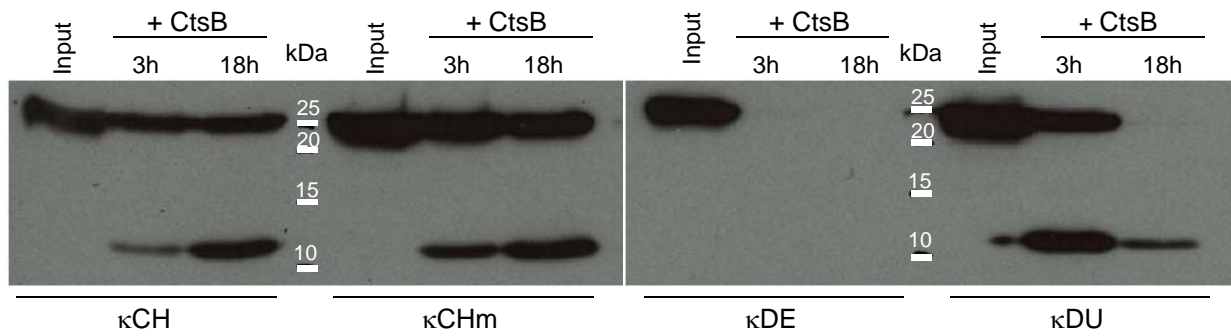


Figure S3

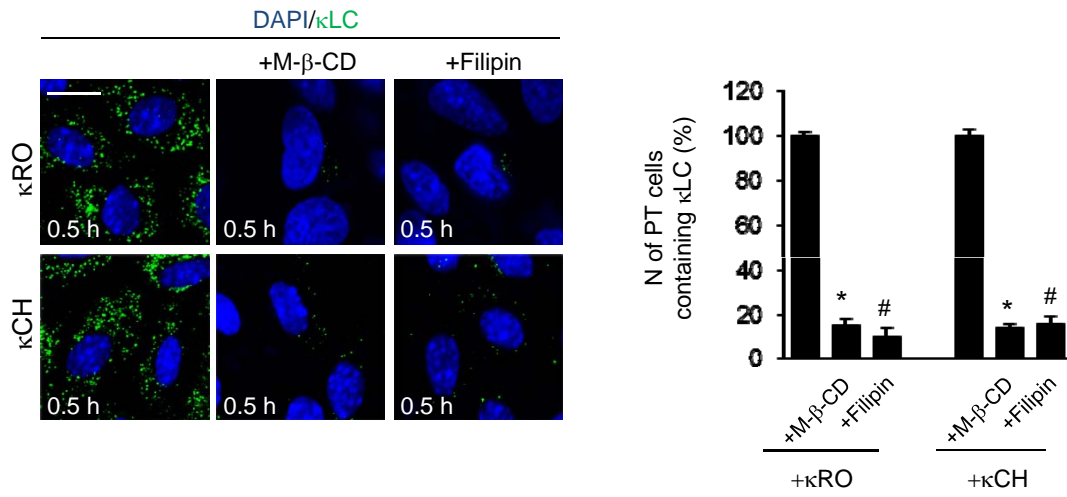


Figure S4

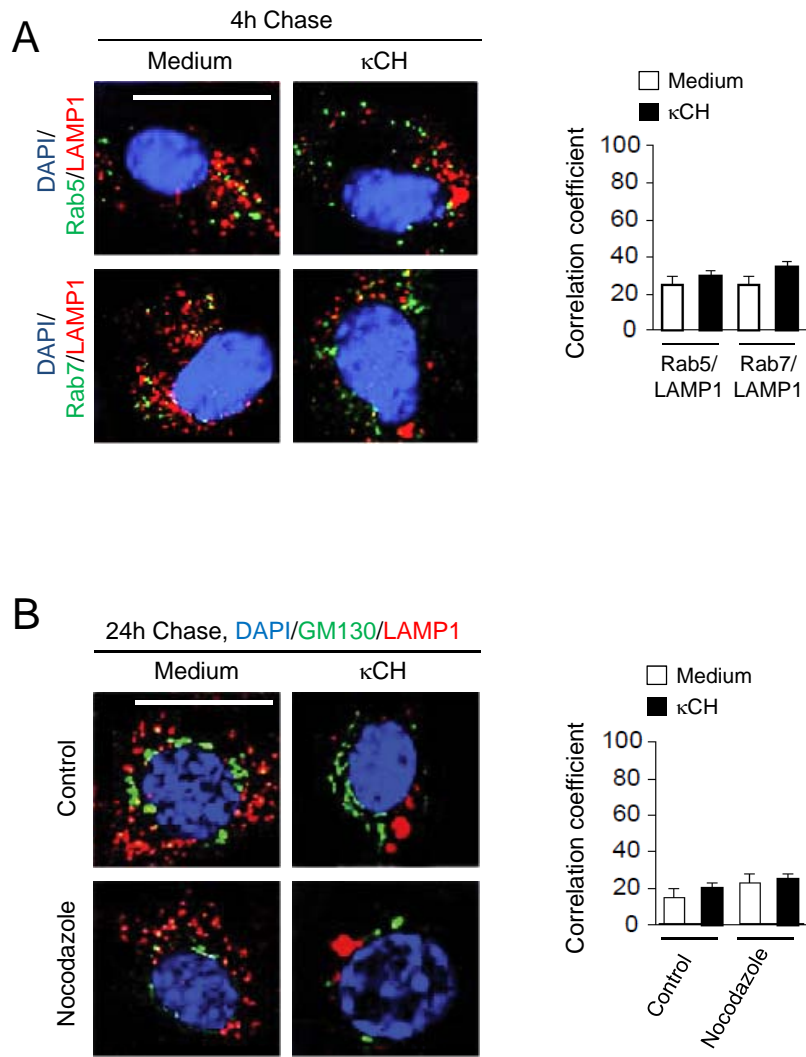


Figure S5

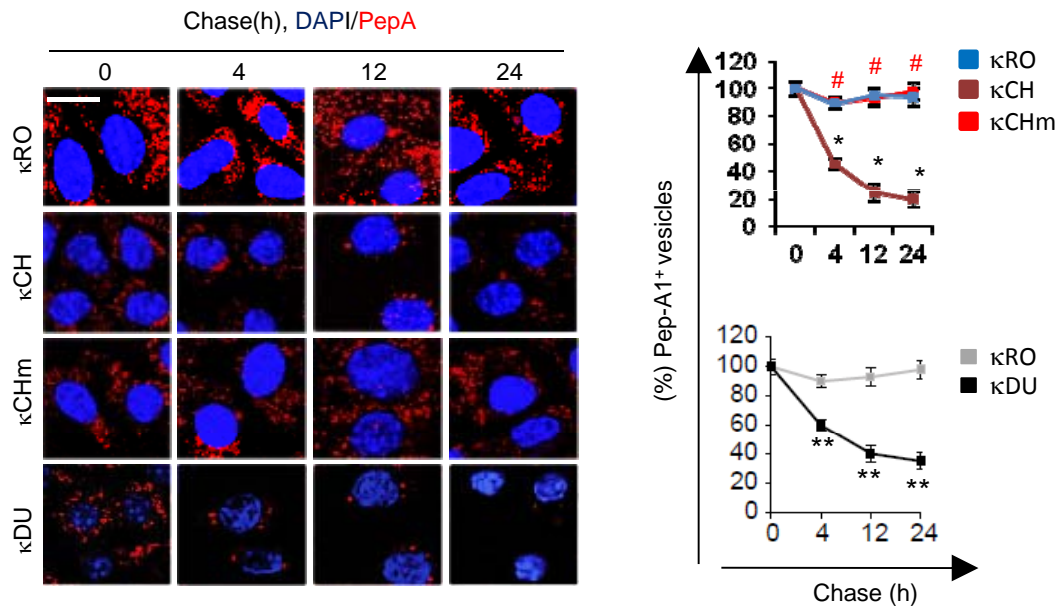


Figure S6

